Colloquia: La Thuile 2016

The DarkSide physics program and its recent results

D. D'Angelo(28)(27)(*), P. Agnes(1), L. Agostino(24),
I. F. M. Albuquerque(36)(44), T. Alexander(42)(13), A. K. Alton(4),
K. Arisaka(41), H. O. Back(35), B. Baldin(13), K. Biery(13), G. Bonfini(3),
M. Bossa(2)(3), B. Bottino(15)(14), A. Brigatti(27), J. Brodsky(36),
F. Budano(37)(38), S. Bussino(37)(38), M. Cadeddu(9)(7), L. Cadonati(42),
M. Cadoni(9)(7), F. Calaprice(36), N. Canci(17)(3), A. Candela(3),
H. Cao(36), M. Cariello(14), M. Carlini(3), S. Catalanotti(31)(30),
P. Cavalcante(3), A. Chepurnov(29), A. G. Cocco(30), G. Covone(31)(30),
L. Crippa(28)(27), M. D'Incecco(3), S. Davini(2)(3), S. De Cecco(24),
M. De Deo(3), M. De Vincenzi(37)(38), A. Derbin(32), A. Devoto(9)(7),
F. Di Eusanio(36), G. Di Pietro(3)(27), E. Edkins(16), A. Empl(17),
A. Fan(41), G. Fiorillo(31)(30), K. Fomenko(12), G. Forster(42)(13),
D. Franco(1), F. Gabriele(3), C. Galbiati(36)(3), C. Giganti(24),
A. M. Goretti(3), F. Granato(40), L. Grandi(10), M. Gromov(29),
M. Guan(18), Y. Guardincerri(13), B. R. Hackett(16), K. Herner(13),
E. V. Hungerford(17), Al. Ianni(25)(3), An. Ianni(36)(3), I. James(37)(38),
C. Jollet(19), K. Keeter(6), C. L. Kendziora(13), V. Kobychev(20), G. Koh(36),
D. Korablev(12), G. Korga(17)(3), A. Kubankin(5), M. Lissia(7), X. Li(36),
P. Lombardi(27), S. Luitz(39), I. N. Machulin(22)(26), A. Mandarano(2)(3),
J. Maricic(16), L. Marini(15)(14), S. M. Mari(37)(38), C. J. Martoff(40),
Y. Ma(18), A. Meregaglia(19), P. D. Meyers(36), T. Miletic(40),
R. Milincic(16), D. Montanari(13), A. Monte(42), M. Montuschi(3),
M. Monzani(39), P. Mosteiro(36), B. J. Mount(6), V. N. Muratova(32),
P. Musico(14), J. Napolitano(40), A. Nelson(36), S. Odrowski(3), M. Orsini(3),
F. Ortica(34)(33), L. Pagani(15)(14), M. Pallavicini(15)(14), E. Pantic(11),
S. Parmeggiano(27), K. Pelczar(21), N. Pelliccia(34)(33), S. Perasso(1),
A. Pocar(42)(36), S. Pordes(13), D. A. Pugachev(22)(26), H. Qian(36),
K. Randle(36), G. Ranucci(27), A. Razeto(3)(36), B. Reinhold(16),
A. L. Renshaw(17)(41), A. Romani(34)(33), B. Rossi(30)(36), N. Rossi(3),
D. Rountree(45), D. Sablone(3), P. Saggese(27), R. Saldanha(10),
W. Sands(36), S. Sangiorgio(23), C. Savarese(2)(3), E. Segreto(8),
D. A. Semenov(32), E. Shields(36), P. N. Singh(17), M. D. Skorokhvatov(22)(26),
O. Smirnov(12), A. Sotnikov(12), C. Stanford(36), Y. Suvorov(41)(3)(22),
R. Tartaglia(3), J. Tatarowicz(40), G. Testera(14), A. Tonazzo(1),
P. Trinchese(31), E. V. Unzhakov(32), A. Vishneva(12), B. Vogelaar(45),
M. Wada(36), S. Walker(31)(30), H. Wang(41), Y. Wang(18)(41),
A. W. Watson(40), S. Westerdale(36), J. Wilhelmi(40), M. M. Wojcik(21),
X. Xiang(36), J. Xu(36), C. Yang(18), J. Yoo(13), S. Zavatarelli(14), A. Zec(42),
W. Zhong(18), C. Zhu(36) and G. Zuzel(21)

(*) E-mail: davide.dangelo@mi.infn.it

1

2

(^{1}) *APC, Université Paris Diderot, CNRS/IN2P3, CEA/Irfu, Obs. de Paris, Sorbonne Paris Cité - Paris 75205, France*
(^{2}) *Gran Sasso Science Institute - L'Aquila AQ 67100, Italy*
(^{3}) *Laboratori Nazionali del Gran Sasso - Assergi AQ 67010, Italy*
(^{4}) *Department of Physics and Astronomy, Augustana University - Sioux Falls, SD 57197, USA*
(^{5}) *Radiation Physics Laboratory, Belgorod National Research University - Belgorod 308007, Russia*
(^{6}) *School of Natural Sciences, Black Hills State University - Spearfish, SD 57799, USA*
(^{7}) *Istituto Nazionale di Fisica Nucleare, Sezione di Cagliari - Cagliari 09042, Italy*
(^{8}) *Institute of Physics Gleb Wataghin, Universidade Estadual de Campinas - São Paulo 13083-859, Brazil*
(^{9}) *Department of Physics, Università degli Studi - Cagliari 09042, Italy*
(^{10}) *Kavli Institute, Enrico Fermi Institute, and Dept. of Physics, University of Chicago Chicago, IL 60637, USA*
(^{11}) *Department of Physics, University of California - Davis, CA 95616, USA*
(^{12}) *Joint Institute for Nuclear Research - Dubna 141980, Russia*
(^{13}) *Fermi National Accelerator Laboratory - Batavia, IL 60510, USA*
(^{14}) *Istituto Nazionale di Fisica Nucleare, Sezione di Genova - Genova 16146, Italy*
(^{15}) *Department of Physics, Università degli Studi - Genova 16146, Italy*
(^{16}) *Department of Physics and Astronomy, University of Hawaií - Honolulu, HI 96822, USA*
(^{17}) *Department of Physics, University of Houston - Houston, TX 77204, USA*
(^{18}) *Institute of High Energy Physics - Beijing 100049, China*
(^{19}) *IPHC, Université de Strasbourg, CNRS/IN2P3 - Strasbourg 67037, France*
(^{20}) *Institute for Nuclear Research, National Academy of Sciences of Ukraine - Kiev 03680, Ukraine*
(^{21}) *Smoluchowski Institute of Physics, Jagiellonian University - Krakow 30348, Poland*
(^{22}) *National Research Centre Kurchatov Institute -Moscow 123182, Russia*
(^{23}) *Lawrence Livermore National Laboratory, Livermore - CA 94550, USA*
(^{24}) *LPNHE Paris, Université Pierre et Marie Curie, Université Paris Diderot, CNRS/IN2P3 Paris 75252, France*
(^{25}) *Laboratorio Subterráneo de Canfranc - Canfranc Estación 22880, Spain*
(^{26}) *National Research Nuclear University MEPhI - Moscow 115409, Russia*
(^{27}) *Istituto Nazionale di Fisica Nucleare - Sezione di Milano, Milano 20133, Italy*
(^{28}) *Department of Physics, Università degli Studi - Milano 20133, Italy*
(^{29}) *Skobeltsyn Institute of Nuclear Physics, Lomonosov Moscow State University - Moscow 119991, Russia*
(^{30}) *Istituto Nazionale di Fisica Nucleare, Sezione di Napoli - Napoli 80126, Italy*
(^{31}) *Department of Physics, Università degli Studi Federico II - Napoli 80126, Italy*
(^{32}) *St. Petersburg Nuclear Physics Institute NRC Kurchatov Institute - Gatchina 188350, Russia*
(^{33}) *Istituto Nazionale di Fisica Nucleare, Sezione di Perugia - Perugia 06123, Italy*
(^{34}) *Department of Chemistry, Biology and Biotechnology, Università degli Studi - Perugia 06123, Italy*
(^{35}) *Pacific Northwest National Laboratory - Richland, WA 99354, USA*
(^{36}) *Department of Physics, Princeton University - Princeton, NJ 08544, USA*
(^{37}) *Istituto Nazionale di Fisica Nucleare, Sezione di Roma Tre - Roma 00146, Italy*
(^{38}) *Department of Physics and Mathematics, Università degli Studi Roma Tre - Roma 00146, Italy*
(^{39}) *SLAC National Accelerator Laboratory - Menlo Park, CA 94025, USA*
(^{40}) *Department of Physics, Temple University - Philadelphia, PA 19122, USA*
(^{41}) *Department of Physics and Astronomy, University of California - Los Angeles, CA 90095, USA*
(^{42}) *Amherst Center for Fundamental Interactions and Dept. of Physics, University of Massachusetts - Amherst, MA 01003, USA*
(^{43}) *University of Crete - Rethymno 74100, Greece*
(^{44}) *Instituto de Física, Universidade de São Paulo - São Paulo 05508-090, Brazil*
(^{45}) *Department of Physics, Virginia Tech - Blacksburg, VA 24061, USA*

Summary. — DarkSide (DS) at Gran Sasso underground laboratory is a direct Dark Matter search program based on Time Projection Chambers (TPC) with liquid Argon from underground sources. The DarkSide-50 (DS-50) TPC, with 150 kg of Argon is installed inside active neutron and muon detectors. DS-50 has been taking data since November 2013 with Atmospheric Argon (AAr) and since April 2015 with Underground Argon (UAr), depleted in radioactive ^{39}Ar by a factor ~ 1400. The exposure of 1422 kg d of AAr has demonstrated that the operation of DS-50 for three years in a background free condition is a solid reality, thanks to the superb performance of the Pulse Shape Analysis. The first release of results from an exposure of 2616 kg d of UAr has shown no candidate Dark Matter events. We have set the best limit for Spin-Independent elastic nuclear scattering of WIMPs obtained by Argon-based detectors, corresponding to a cross-section of $2\,10^{-44}\,\mathrm{cm}^2$ at a WIMP mass of 100 GeV. We present the detector design and performance, the results from the AAr run and the first results from the UAr run and we briefly introduce the future of the DarkSide program.

1. – The DarkSide program

The DarkSide (DS) project [1] aims to direct Dark Matter detection via WIMP-nucleus scattering in liquid Argon. The detectors are dual phase Time Projection Chambers (TPC) located at Laboratori Nazionali del Gran Sasso in central Italy under a rock coverage of ~ 3800 m w.e. DS aims to a background-free exposure via three key concepts: 1) very low intrinsic background levels, 2) discrimination of electron recoils and 3) active suppression of the neutron background.

We are currently operating the DarkSide-50 (DS-50) detector with a 45 kg fiducial mass TPC since the end of 2013. We present here the results of the Atmospheric Argon (AAr) phase of 2014 and of the first exposure with Underground Argon (UAr). DS-50 is expected to continue data taking up to the end of 2017. The project will continue with DarkSide-20k (DS-20k) a multi-ton detector with an expected sensitivity improvement of two orders of magnitude.

2. – The DS-50 TPC

The DS-50 TPC is depicted in fig. 1. The scattering of WIMPs or background particles in the active volume induces a prompt scintillation light, called S1, and ionization. Electrons which do not recombine are drifted by an electric field applied along the z-axis. The maximum drift time across the 35.6 cm height is $\sim 375\,\mu$s at the operative field of 200 V/cm. Electrons are then extracted into gaseous argon above the extraction grid, by an extraction field of 4200 V/cm. Here a secondary larger signal due to electroluminescence takes place, called S2. After circulating Argon through charcoal filters for about 5 months, the electron lifetime was brought a stable value of ~ 5 ms, much larger then
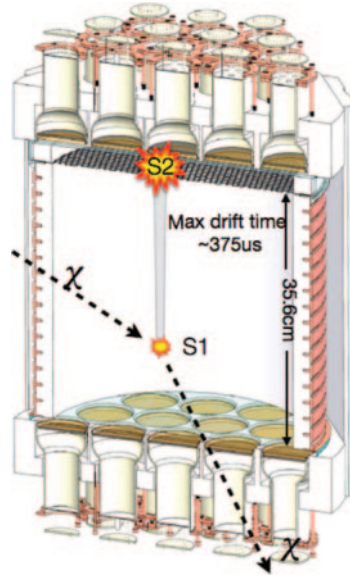
Fig. 1. – DS-50 TPC principle of operation.

the maximum drift time. The light is collected by two arrays of 19 3″-PMTs on each side of the TPC corresponding to a 60% geometrical coverage of the end plates and 20% of the total TPC surface. The detector is capable of reconstructing the position of the interaction in 3D. The z-coordinate is easily computed by the drift time, while the time profile of the S2 light collected by the top plate PMTs allows to reconstruct the x- and y-coordinates.

3. – The DS-50 neutron and muon detectors

As can be seen in fig. 2, the TPC is housed inside an organic liquid scintillator Neutron Detector (ND) and a water Cherenkov Muon Detector (MD) [2]. The ND is made by
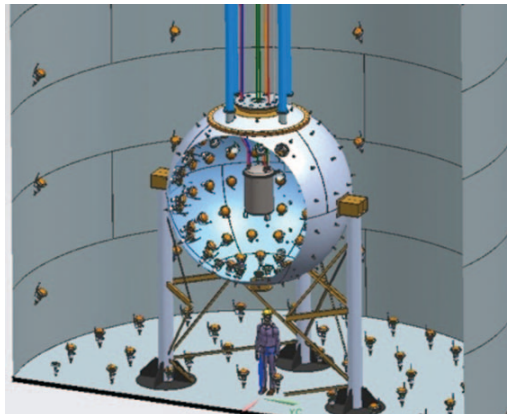

Fig. 2. – DS-50 Schematics. TPC, ND and MD are visible.

a 4 m diameter steel sphere filled with a mixture of Pseudocumene (PC), doped with PPO, and Trimethyl Borate (TMB) for enhanced neutron detection. The scintillation light is captured by 110 8″-PMTs mounted on the sphere's inner surface. It also features independent trigger capabilities for an in-situ measurement of the neutron background. Boron has a high n-capture cross section which allows a compact veto size and reduces the capture time to $2.3\,\mu s$ or $22.2\,\mu s$ at 50% and 5% TMB concentration, respectively. For comparison, the neutron capture time in pure PC was measured to be $\sim 255\,\mu s$ [3]. The n-capture on ^{10}B results in recoiling ^{7}Li and α particle. In 94% of the cases a $0.48\,$MeV-γ accompanies the process and is brightly visible. In the remaining cases the recoil energy of 1.47 MeV must be detected and this is typically quenched to $\sim 50\,$keV. The ND was first filled at the end of 2013 with PC and TMB at 50% concentration and fully commissioned. The LY has been found to be $\sim 0.5\,$pe/keV, sufficient to detect the Li and α recoil energy. Unfortunately we have observed a high rate, about 150 kBq, due to the intrinsic biogenic isotope ^{14}C in the TMB, at the level of $\sim 10^{-13}\,$g/g. The capability of rejecting neutrons that leave a signal also in the TPC was consequently about 98%, not fully meeting the design goal of 99.5%. We have therefore replaced TMB with pure Pseudocumene and procured TMB from an oil batch with ^{14}C below $10^{-15}\,$g/g. In January 2015 we have loaded TMB from this new batch in the detector to a concentration of 5% for the upcoming UAr campaign, with a resulting activity of about 0.3 kBq.

The MD is a cylindrical tank, 11 m in diameter and 10 m high, filled with ultra-pure water and instrumented with 80 8″-PMTs on the floor and inner walls. In addition of acting as a water Cherenkov detector for through-going muons with $> 99\%$ efficiency, it also serves as passive shielding against gammas and neutrons from the rocks.

4. – The ^{39}Ar problem

Operating Argon detectors implies dealing with the intrinsic cosmogenic background from ^{39}Ar, a β-emitter with $Q = 565\,$keV and $\tau_{1/2} = 269\,$y. In Atmospheric Argon (AAr) its activity can be as high as $\sim 1\,$Bq/kg. We have identified a source of Underground Argon (UAr) in a mine in Colorado (USA), where the activity was evaluated to be $< 6.5\,$mBq/kg from in-situ measurements. At Fermi National Laboratory (USA) we operate a cryogenic distillation plant able to produce the UAr at a rate of $\sim 0.5\,$kg/d. In addition of pursuing a target material with the lowest possible content of ^{39}Ar, we also exploit Pulse Shape Discrimination to identify this source of background. Argon has an intrinsic capability to distinguish Electron Recoils (ER) such as ^{39}Ar decays from Nuclear Recoils (NR). Prompt scintillation light in Argon comes from the de-excitation of singlet and triplet states of Ar_2^*, having very different mean lives: $\tau_{\text{singlet}} \sim 7\,$ns while $\tau_{\text{triplet}} \sim 1.6\,\mu s$. Since NRs tend to populate more the singlet state, they result in significantly faster signals compared to ERs. We define the parameter F90 as the ratio of the charge collected in the first 90 ns over the total S1 charge. NRs are distributed around F90 ~ 0.7 while ERs around F90 ~ 0.3.

5. – DS-50 performance and calibration

We have characterised our detector in terms of Light Yield (LY) [4]. At null field we have obtained the LY from the ^{39}Ar shoulder at 565 keV. $LY_{\text{null}} = 8.1 \pm 0.2\,$pe/keV, assumed energy independent within 3%. With the application of the drift field, the LY becomes energy dependent and ^{39}Ar is way beyond our region of interest. Therefore we
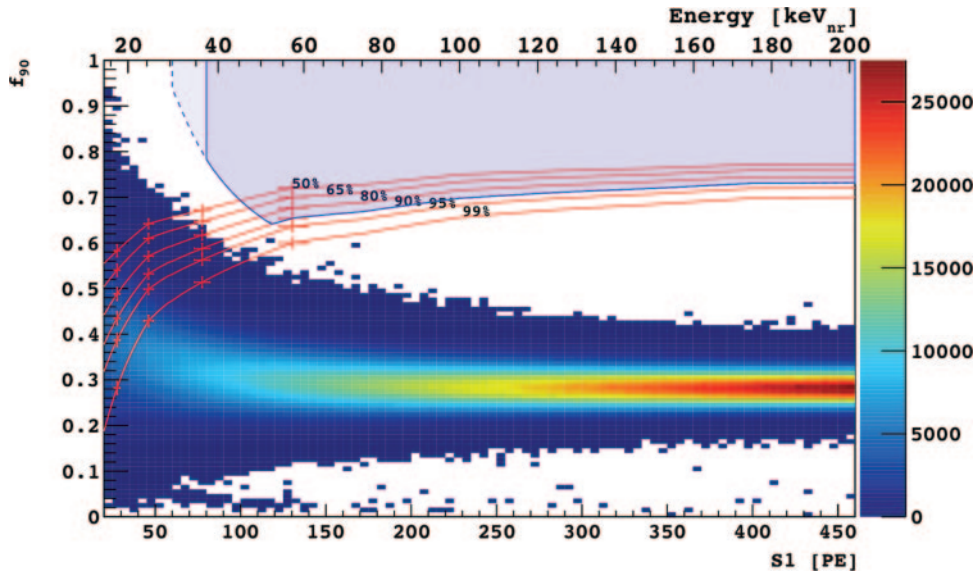
Fig. 3. – Atmospheric Argon exposure of 1422 ± 67 kg-days, F90 *vs.* S1 energy in photoelectrons (PE) units with the NR acceptance curves and the WIMP search region superimposed.

periodically spike the argon by adding gaseous ^{83m}Kr in the recirculation system. ^{83m}Kr decays fast ($\tau_{1/2} \sim 1.8$ h) and yields a monochromatic line at 41.5 keV. We have used the relative position of this line with and without drift field to scale the LY, obtaining $LY_{200V} = 7.0 \pm 0.3$ pe/keV at 200 V/cm.

Compared to ERs, NRs are quenched by a factor that depends on energy and field. We have used the data from the SCENE [5] experiment at University of Notre Dame (USA) to study the detector response to nuclear recoils. SCENE features a small TPC with a concept similar to DS exposed to a neutron beam whose energy can be selected. SCENE has measured quenching factors at different neutron energies and drift fields with respect to ERs from ^{83m}Kr decays. We have processed SCENE raw data using the DS reconstruction code and we have obtained the quenching factors as well as the distributions of the F90 parameter.

At the end of 2014 we have also calibrated the detector using radioactive sources mounted on the tip of a segmented arm and inserted in the ND volume through a service port about 1 m off-axis. The arm includes a movable joint that allows to bring the source in direct contact with the cryostat. We have used three gamma sources, ^{57}Co (122 keV), ^{133}Ba (356 keV) and ^{137}Cs (633 keV) to tune the energy response in the Monte Carlo code. We have also used a neutron ^{241}Am-Be source to cross-check the F90 distribution obtained from SCENE data, obtaining consistent results.

6. – Atmospheric Argon results

Around 2014 we acquired about one year of data with AAr. In fig. 3 are shown events corresponding to 1422 ± 67 kg-days in the parameter plane of F90 *vs.* S1 energy in photoelectrons [4]. Only single-hit events are selected. A *z*-cut is applied to remove the regions close to the cathode and to the extraction grid. Events which show a coincident energy deposition in the ND are removed. In this energy scale 70 pe and 125 pe correspond
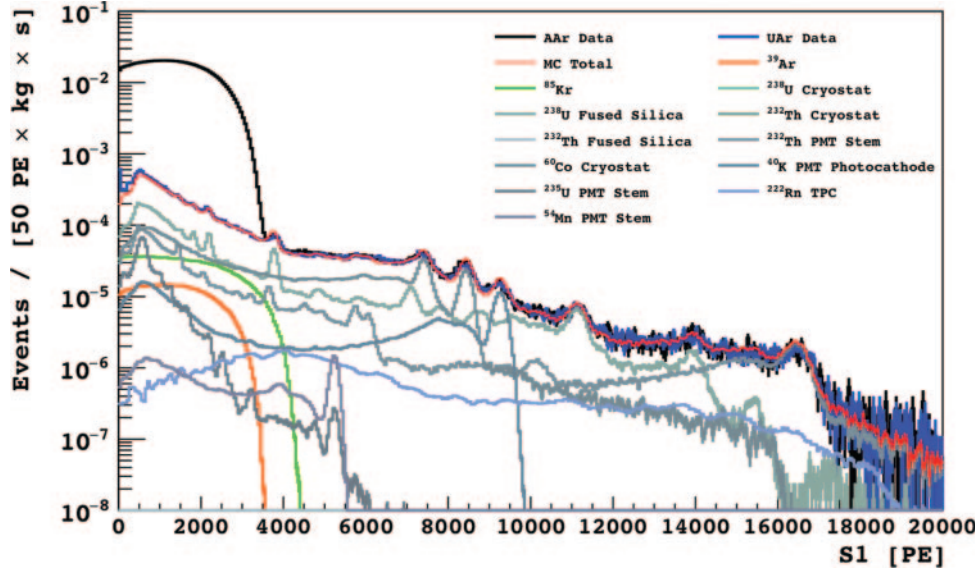
Fig. 4. – Energy spectrum of Underground Argon in photoelectrons (PE). Atmospheric Argon spectrum normalized for the same exposure is also shown for comparison as well as MC simulation of backgrounds.

to $\sim 35 \, \text{keV}$ and $\sim 57 \, \text{keV}$ NRs according to the quenching factors determined from the SCENE data. We have set our energy threshold for WIMP searches at 80 pe. We have also superimposed the F90 NR acceptance curves derived from SCENE. We have defined a WIMP search region as in fig. 3 and observed no events within. This exposure contains the same ^{39}Ar events of 38.7 y of operation at a contamination as high as the one observed in UAr (below). We therefore prove that the we can efficiently suppress the dominant ER background that we expect in the full DS-50 UAr run (three years), while maintaining a high acceptance for WIMPs.

7. – Underground Argon results

In April 2015 we have filled DS-50 with UAr [6]. The full energy spectrum at null drift field can be seen in fig. 4 in blue. The AAr spectrum is also shown in black for comparison, after scaling to the same exposure. As can be seen the ^{39}Ar shoulder prominent in the low energy part of the spectrum for AAr is no longer present in UAr data. The results from a Monte Carlo simulation of all known backgrounds is shown in red and reproduces the data closely. The activity due to ^{39}Ar (orange line) is now lower by a factor ~ 1400, about one order of magnitude better then our expectations. In fact the background in the low energy part of the spectrum, where the WIMP search region is located, is smaller by a factor ~ 300 and is now dominated by contaminations in the cryostat and in the fused silica windows behind which the PMTs are located (different grey lines). A contribution from internal ^{85}Kr is also evidenced (green line). This very promising result demonstrates that scaling the liquid Argon technology to a background-free multi-ton detector is possible.
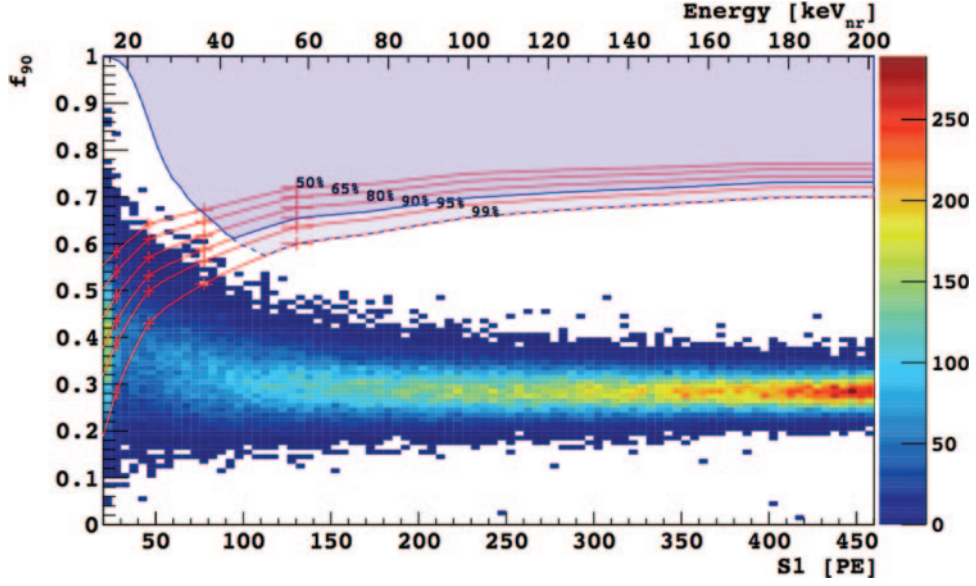
Fig. 5. – Underground Argon exposure of 2616 ± 43 kg-days, F90 *vs.* S1 energy in photoelectrons (PE) units with the NR acceptance curves and the WIMP search region superimposed.
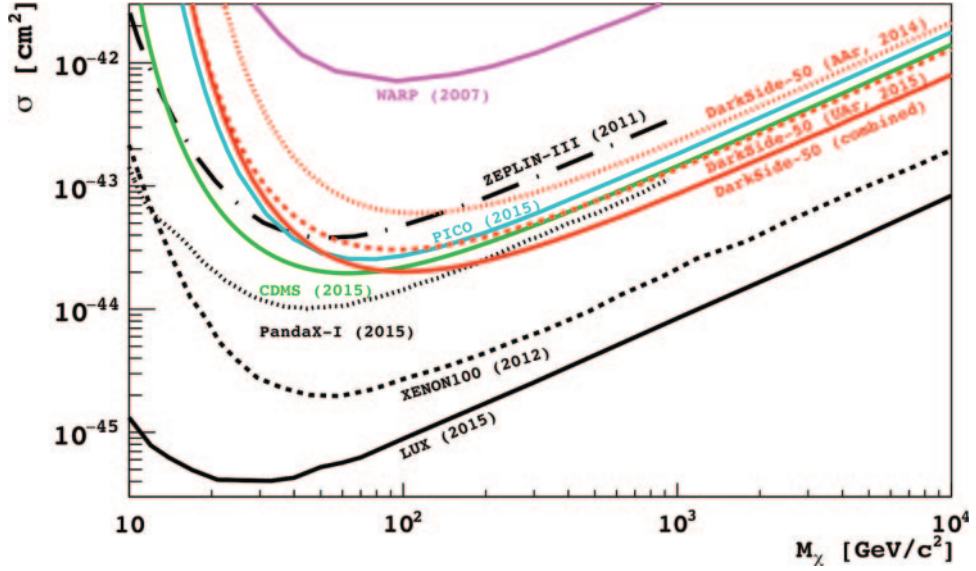

Fig. 6. – Parameters' plane for spin-independent WIMP-nucleon interaction. Most recent exclusion curves in the high mass region are shown. DS-50 limits are shown in red.

Figure 5, analogous to fig. 3, presents the result of the first UAr run, corresponding to an exposure of 2616 ± 43 kg-day. The same cuts described above apply. The WIMP search region is defined by the shaded area and no events are found within.

8. – Limits on WIMP parameters

Figure 6 shows the parameters plane [WIMP mass, WIMP-nucleon cross section] for spin-independent interactions. The limit that can be inferred by the non observation of events in the WIMP search region in DS-50 are shown in red and compared to the most recent results from other experiments. The dotted/dashed line correspond the AAr/UAr runs, while the solid line arises from the combination on the two exposures [6]. This is today the best limit obtained with an Argon detector. At the end of its planned three years campaign, DS-50 will be able to lower this limit to a WIMP-nucleon cross-section of about $2 \times 10^{-45}\,\mathrm{cm}^2$ for a WIMP of $100\,\mathrm{GeV}$ mass.

9. – The future of DarkSide

The DarkSide program will continue with DarkSide-20k (DS-20k) and Argo, with 30t (20t FV) and 300t (200t FV) of liquid argon, respectively. While Argo is currently being designed, DS-20k is expected to start data taking in 2020. The optical sensors will be SiPM matrices with very low radioactivity, while the cryostat might be fabricated out of ultra clean Titanium to limit the sources of background currently dominating the low energy region of DS-50 (see fig. 4). Further suppression of external background will be achieved with x-y fiducialization which is not yet applied in DS-50. However the goal of DS-20k is a background free exposure of 100 ton-year which requires further suppression of ^{39}Ar background with respect to DS-50. The project Urania involves the upgrade of the UAr extraction plant to a production rate of about $100\,\mathrm{kg/d}$, suitable for multi-ton detectors. The project Aria instead involves the construction of a very tall cryogenic distillation column in the Seruci mine (Sardinia, Italy) with the high-volume capability of chemical and isotopic purification of UAr. The projected sensitivity of DS-20k and Argo reaches a WIMP-nucleon cross-section of $10^{-47}\,\mathrm{cm}^2$ and $10^{-48}\,\mathrm{cm}^2$ respectively, for a WIMP mass of $100\,\mathrm{GeV}$, exploring the region of the parameters plane down to the irreducible background due to atmospheric neutrinos.

REFERENCES

[1] DARKSIDE COLLABORATION (T. ALEXANDER et al.), JINST, **8** (2013) C11021.
[2] DARKSIDE COLLABORATION (P. AGNES et al.), J. Instrum., **11** (2016) P03016.
[3] BOREXINO COLLABORATION (G. BELLINI et al.), JCAP, **08** (2013) 049.
[4] DARKSIDE COLLABORATION (P. AGNES et al.), Phys. Lett. B, **743** (2015) 456.
[5] SCENE COLLABORATION (H. CAO et al.), Phys. Rev. D, **91** (2015) 092007.
[6] DARKSIDE COLLABORATION (P. AGNES et al.), Phys. Rev. D, **93** (2016) 081101.